# Structures of inorganic polymers in sol-gel processes based on titanium oxide

M. Kallala

*Equipe Mixte Commissariat à l'Energie Atomique–Rhône-Poulenc, Service de Chimie Moléculaire,*
*Centre d'Etudes Nucléaires de Saclay, 91191 Gif sur Yvette Cedex, France*

C. Sanchez

*Laboratoire de Chimie de la Matière Condensée, Université Pierre et Marie Curie, 75252 Paris, France*

B. Cabane

*Equipe Mixte Commissariat à l'Energie Atomique–Rhône-Poulenc, Service de Chimie Moléculaire,*
*Centre d'Etudes Nucléaires de Saclay, 91191 Gif sur Yvette Cedex, France*

Inorganic gels and precipitates have been made through hydrolysis and condensation of the precursor $Ti(OBu^n)_4$ dissolved in $n$-butanol. The condensation of uninhibited precursors leads to precipitation; the selective inhibition of condensation through $H^+$ ions prevents precipitation and leads to gelation. The structures of the polymers which result from condensation in either case have been examined through small-angle x-ray scattering. It has been found that these structures vary continuously with the inhibition ratio. At high inhibition, the polymers are tenuous objects with a self-similarity exponent $d_f \approx 2$; they invade the whole sample volume to form transparent gels. At intermediate ratios, the polymers become bushy with a self-similarity exponent $d_f > 2$ and they form turbid gels. Finally, precipitation occurs when $d_f$ reaches 3. These nonuniversal values of the exponents result from nonstationary growth modes, where a few large polymers grow first, and then densify through the capture of unused monomers.

PACS number(s): 82.70.Gg, 82.35.+t

## INTRODUCTION

Sol-gel processes are a way to make dispersed materials through the growth of inorganic polymers in a solvent [1]. The starting point is a solution of metallo-organic precursors in an alcohol. First these precursors are hydrolyzed into monomers which carry four reactive functions each. Then the monomers condense to form branched polymers with an oxide skeleton and reactive hydroxyls as side groups. The recombination of these polymers produces bushy structures which invade the whole volume. When these polymers reach macroscopic sizes, the reaction bath becomes a gel; the solvent, reaction byproducts, and free polymers are trapped in this gel [2–4]. Later on, the gel may be used as a host for active species, or evacuated to yield a porous material, or collapsed to yield films or fibers [1]. The success of these operations depends on the structures of the polymers, which must be controlled. This paper is about the structures of the growing polymers, and how they can be controlled.

The general idea is that control is achieved through changes in the conditions of the reactions. Indeed a *gel* is not the only possible outcome for such polymerization reactions. Other final states may be reached, including *sols* where the polymerized structure did not reach macroscopic sizes, and *precipitates* where the reactions produce dense structures rather than bushy ones [5,6]. The gels may also differ according to the conditions of the reaction, some being more lumpy or with a larger mesh size than others. This variability comes from the many different ways in which monomers can be linked and organized when they are dispersed in a solvent.

The range of evolutions is particularly important for polymers based on transition-metal oxides. Indeed the precursors, transition-metal alkoxides (TMA), are highly reactive species [7]. The normal course of the reaction for TMA dissolved in a solvent leads to precipitation of the polymers out of the solvent. Thus control of the reactivity of TMA is necessary in order to obtain sols and gels where the polymers remain swollen by the solvent. This control may be achieved through the addition of "modifiers" such as $\beta$-diketones, carboxylic acids, or other complexing ligands which act as termination groups for condensation [8,9]. Addition of such inhibitors can prevent precipitation, force the growth to end in a gel state, or stop growth altogether. This is usually explained by an effect of the ligands on the average functionality of monomers. However, large changes in structures are obtained at rather low modification ratios, typically 0.1 ligand per metal. It is hard to believe that such a modest change in average functionality would have drastic consequences on the large scale structures of the polymers. No satisfactory explanation for this mechanism is found in the sol-gel literature; however, it does appear to be general, and it does provide an empirical control of the structures.

The simplest inhibitors for condensation reactions are protons ($H^+$ ions). According to their concentration, nucleophilic species (Ti-OH) can be protonated or depro-

tonated, causing selective inhibition of some condensa-tion reactions [10,11]; it has been found that different in-hibition ratios lead to sols, transparent gels, turbid gels, or precipitates [5,6]. In this work we studied the effect of $H^+$ ions on the growth of titanium oxopolymers. In each case we measured the final structures of the polymers in gels made in different reaction conditions according to (a) the hydrolysis ratio which determines the potential func-tionality of monomers; (b) the inhibition ratio which selects the relative rates of different reactions; (c) the monomer concentration, which determines how large the polymers can grow before they get in each other's way.

## PRECURSORS

As in many sol-gel processes the precursors are metal alkoxides. For titanium oxopolymers, classical precur-sors are the $n$-butoxide $Ti(OBu^n)_4$ and the isopropoxide $Ti(OPr^i)_4$. In such alkoxide precursors the oxidation state of the metal is smaller than its preferred coordina-tion number. Consequently the metal will tend to in-crease its coordination by using its vacant $d$ orbitals for accepting oxygen or nitrogen lone pairs from nucleophil-ic ligands. Typical nucleophiles are oxygen atoms from water, from hydroxy or alkoxy groups, or even from sol-vating alcohol molecules; consequently the precursors tend to react with almost anything. In the absence of wa-ter and at room temperature the pure precursors are stable. We bought these precursors from Fluka and used them without further purification; however, it was neces-sary to use fresh bottles only, as moisture causes the al-koxide to polymerize over time.

The organization of precursor molecules in the pure liquid state was examined through SAXS. Figure 1 shows the spectra of the pure alkoxides. The peaks cor-respond to the repetition of identical units in the liquid. For the isopropoxide the peak position yields a real space distance $d = 8.5$ Å. This is quite close to the average dis-
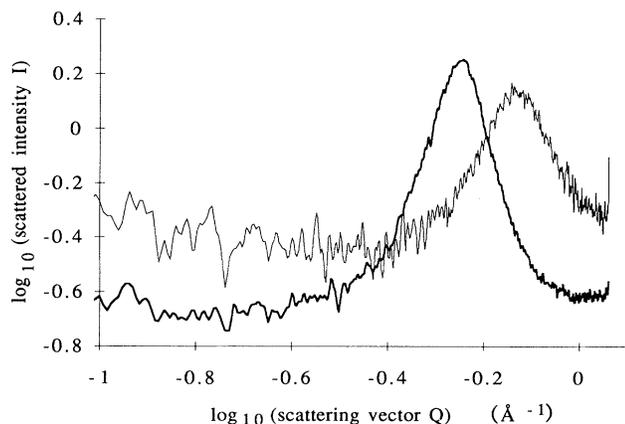


FIG. 1. SAXS spectra of the pure alkoxides. Horizontal axis: scattering vector $Q$, $\log_{10}$ scale. Vertical axis: scattered intensity, $\log_{10}$ scale. Thin line: spectrum of the pure isopro-poxide; in this case the peak corresponds to a distance between monomers. Thick line: spectrum of the pure $n$-butoxide; in this case the peak corresponds to a distance between trimers.

tance between isopropoxide molecules in a simple cubic packing, which is 8.27 Å. Hence in $Ti(OPr^i)_4$ the only re-peat unit is the individual molecule. For the $n$-butoxide the peak position yields a real space distance $d = 11.5$ Å. This is substantially larger than the average distance be-tween individual molecules. Actually the measured dis-tance is close to that calculated for a liquid made ex-clusively of trimers, which is 11.9 Å. Hence the precur-sor $Ti(OBu^n)_4$ in the liquid state must be associated in tri-mers. This association had already been demonstrated for precursors in the liquid state or dissolved in a non-nucleophilic solvent such as benzene or cyclohexane through cryoscopy [7] and through x-ray absorption near-edge structure (XANES) and extended x-ray absorp-tion fine structure (EXAFS) [12] methods.

The cause of the association of $Ti(OBu^n)_4$ in trimers is the discrepancy between the oxidation state of titanium in the alkoxide and its preferred coordination, as men-tioned above. Trimerization occurs through the forma-tion of alkoxy bridges between titanium atoms, thereby increasing the coordination of titanium from 4 to 5, as shown below, where R is the butyl group:



$$(1)$$
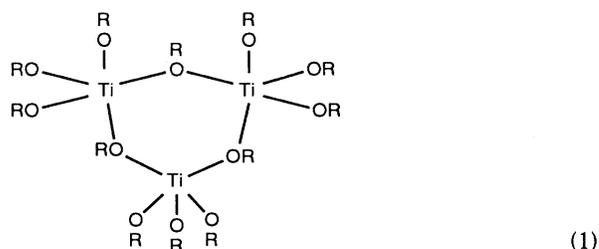
For $Ti(OPr^i)_4$ the oligomerization is prevented by the steric hindrance of the bulkier isopropoxo groups. Discrepancy between the coordination of titanium in the alkoxide precursor and its preferred coordination (sixfold coordination) is also a driving force for hydrolysis and condensation reactions. Consequently the butoxide pre-cursor is less reactive than the isopropoxide. This makes it easier to achieve a homogeneous mixture of the reac-tants at the beginning of the sol-gel process. For this reason most experiments were done with $Ti(OBu^n)_4$ as a precursor. For sol-gel reactions the precursors are dis-solved into the related alcohol, $n$-butanol. In that case primary titanium alkoxides can be solvated by the al-cohol. The reaction bath is then composed of different oligomeric species (trimers, solvated dimers, solvated monomers) in equilibrium [12,13].

## CHEMICAL REACTIONS

Upon addition of water to the precursor, a series of chemical reactions occur which ultimately lead to the formation of oxopolymers. The initial reactions allow the titanium to change its coordination through nucleophilic addition, and they produce oligomers with a temporary set of "ol" bridges. Then come slower substitution reac-tions which build polymers with the permanent oxo skeleton.

### Initial hydrolysis

Initiation of the polymerization is performed through hydroxylation of the alkoxide:

$$\equiv \text{Ti—OR} + \text{HOH} \rightarrow \ \equiv \text{Ti—OH} + \text{R—OH} \ . \qquad (2)$$
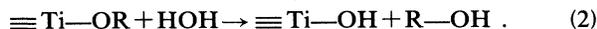
The mechanism occurs in three steps: (a) nucleophilic attack of Ti by a water oxygen; (b) transfer of a water proton to an OR group of the Ti; (c) release of the resulting ROH molecule. In the usual conditions, i.e., precursors dissolved in alcohol and acidic water, all these steps are easy. Step (a) is easy because the titanium atom carries a positive partial charge which attracts the negative partial charge of the water oxygen, and because it has a frustrated coordination; step (b) is facilitated by the presence of $H^+$ ions in the solution, as OR groups tend to pick up protons from the solution; step (c) is immediate since the ROH group becomes a solvating molecule, and solvation energies are low. This first hydrolysis does not increase the coordination of the titanium, hence the hydrolyzed oligomers are still quite reactive.

### Formation of olated polymers

At this stage there is the possibility of increasing the coordination of the titanium through an addition reaction between partially hydrolyzed oligomers. This is an olation reaction where the OH from one Ti atom is added to the coordination sphere of a neighboring Ti atom. In doing so it replaces a solvating ROH molecule which is less strongly bound. The difference in binding energies is revealed by a large release of heat which immediately follows the first hydrolysis reaction.

The occurrence of olation reactions at this stage is supported by abundant experimental evidence. For Ti-based systems, XANES experiments performed immediately after hydrolysis show the rise of a low-intensity triplet in the Ti absorption preedge; this is characteristic of Ti atoms in a sixfold coordination [12]. Hence olation bridges are formed, which raise the coordination of Ti from 4 or 5 to 6. For other tetravalent metal alkoxides the presense of olated products was determined through infrared spectroscopy [14], x-ray diffraction [15], and $^{17}$O NMR spectroscopy [16].

As long as the water-to-alkoxide ratio does not exceed unity, the resulting oligomers are mainly linear, as shown below [17–19]:
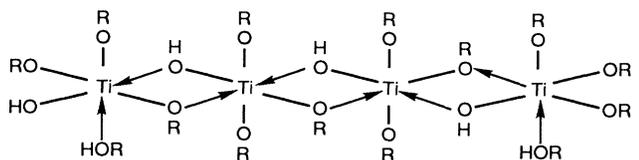


$$(3)$$

When all titanium atoms have increased their coordination in this way the olation reactions must end: indeed there are no more available positions for addition since all solvating molecules have been replaced by OH in

bridging positions. Beyond this stage the system will evolve preferentially through substitution reactions.

### Additional hydrolysis and oxolation

Continuation of the polymerization occurs through a set of nucleophilic substitution reactions: additional hydrolysis (if there is more than one water molecule per Ti atom), where residual OR groups are substituted with OH, and oxolation reactions where OR or OH groups are substituted with OTi bridges. The overall stoichiometry for oxolation is

$$\equiv \text{Ti—O}X + \text{HO—Ti} \equiv \ \rightarrow \ \equiv \text{Ti—O—Ti} \equiv + X\text{OH}$$

$$(X = \text{H or R}) \ . \qquad (4)$$
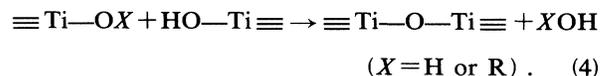
The steps are the same as for hydrolysis: (a) attack of a Ti atom by the O from another TiOH; (b) transfer of the TiOH protons to an OR or OH group of the attacked Ti atom; (c) release of the resulting ROH or HOH molecule. However, the effect of $H^+$ ions on this reaction is not the same as for hydrolysis, and this is essential for the outcome of the polymerization.

Hydrolysis is catalyzed by $H^+$ ions, because step (c), departure of OR groups, is facilitated by proton transfer from the solvent. The same occurs in condensation; yet on the whole condensation is inhibited by $H^+$ ions. This is because step (a) is inhibited by protons. Indeed the approach of the attacking TiOH is slow because it is attached to a bulky polymer. If the medium is acidic, there is a chance that during this approach the TiOH will become protonated. If this occurs, the $\text{TiOH}_2^+$ is repelled, and the attack is aborted. Here the important point is that protonation for a short interval during the approach of TiOH is enough to stop it; because protons are much more mobile than TiOH this can occur very frequently. This does not occur for the attack by a water molecule, which is much faster. *Thus the high mobility of protons compared to TiOH explains why inhibition is efficient even at concentration ratios of $H^+$ to Ti as low as 0.01.*
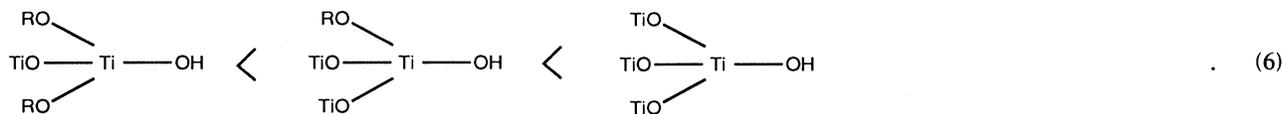
### Selectivity of condensation reactions

From a structural point of view the main question is whether inhibition can be selective, i.e., favor some condensation reactions over others; if it is not selective, then it will only change the rate of the overall reaction and the end products will be the same in all conditions. As indicated above, inhibition occurs through protonation of the attacking TiOH groups; thus the dominant reactions will occur with the TiOH which are least likely to become protonated. That some TiOH are less likely to be pronounced than others is a consequence of the different types of coordinations for the oxygen, as electron charges are displaced by the binding to R or Ti. These differences are known from calculations of partial charges [10] and also from the relative acidities of different sites at oxide surfaces [20]. Accordingly the scale of acid strength is
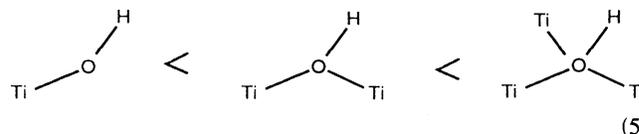


$$(5)$$

Thus bridging oxygens have the strongest acidity, and are the least likely to become protonated. Consequently they are the most likely to react further. Conversely the nonbridging oxygens are more likely to be inhibited;

among them the oxygens at chain ends are the least acidic, again because of displacement of electron charges caused by other bonds to the titanium [10]:

$$
\begin{array}{ccccc}
\text{RO}\diagdown & & \text{RO}\diagdown & & \text{TiO}\diagdown \\
\text{TiO}\text{---}\text{Ti}\text{---}\text{OH} < & & \text{TiO}\text{---}\text{Ti}\text{---}\text{OH} < & & \text{TiO}\text{---}\text{Ti}\text{---}\text{OH} \\
\text{RO}\diagup & & \text{TiO}\diagup & & \text{TiO}\diagup
\end{array}
\qquad . \quad (6)
$$

These differences result in a consistent pattern of selection and inhibition: *previous* condensation reactions favor *further* condensation reactions on the same site. Therefore the growth will occur first in the most condensed regions of the gel.

At high concentrations of $H^+$ this selectivity vanishes because all TiOH are protonated and inhibited to the same extent. Then the rates of different condensation reactions will be determined by steric constraints only [1].

### Reverse reactions

The selection described in Eqs. (5) and (6) has a lasting effect only if the reactions are not reversible. For Ti-based systems, reverse reactions which would break oxo bonds to form smaller polymers are indeed unlikely. Indeed the oxo bonds are extremely strong, and they are not expected to break unless the concentration of $H^+$ is close to that required to dissolve the oxide. Consequently the hierarchy of chemical preferences is trapped at the end of condensation reactions. Thus the outcome of hydrolysis and condensation reactions may be controlled through the ratio of $H^+$ to Ti. The consequences of this selection had already been noticed by Yoldas, who made gels at high ratios of $H^+$ to Ti [5]. The next section presents the effect of this selection on the macroscopic properties of samples according to the ratio $m = [H^+]/[Ti]$.

## GELATION AND PRECIPITATION

### Sample preparation

In this section we present the methods for preparing samples as well as macroscopic observations of the final state of the materials. There are three parameters: the amount $h = [H_2O]/[Ti]$ of water available for hydrolysis, the degree of protonation $m = [H^+]/[Ti]$, and the final concentration [Ti] of monomers in the solvent. These parameters are controlled separately. The main problem in sample preparation is the mixing of the reactants, which was done as follows.

The water used for hydrolysis was acidified with HCl to a set $pH$. Then this water was diluted in $n$-butanol, with a water-to-butanol ratio of $\frac{1}{10}$ in weight. The alkoxide was also diluted in $n$-butanol, to an extent determined by the final concentration desired for the material. The hydrolysis solution was added dropwise to the butoxide solution under high shear; finally the mixture was kept at room temperature, protected from light and moisture.

### Final state of samples at low hydrolysis

The final state of the sample was assessed according to homogeneity, transparency, and mechanical rigidity. Accordingly the samples were labeled into sols, gels, and precipitates. Figure 2 presents the resulting diagram for materials prepared with a hydrolysis ratio $h = 2$. A major finding is that *the final state was determined by the acid-to-alkoxide ratio m* rather than by acid concentration.

For $0 < m < 0.05$ the polymers formed opaque precipitates which expelled the solvent; the rate of precipitation depended on the alkoxide concentration. Some reversibility of the condensation reactions occurring in this regime was observed; indeed precipitates made near the precipitation boundary at $m = 0.05$ tended to swell with solvent and turn to opaque gels; also precipitates could be redissolved in concentrated acids. These observations suggest that a fraction of the bonds made in this regime are weaker "ol" bonds rather than the very strong "oxo" bonds.

For $m > 0.05$ the final products were gels; these gels differed according to the value of $m$. Gels made near the precipitation boundary were hard, friable, and turbid; at times much longer than the gel time these samples tended to expel some solvent (syneresis). Gels made at increasing values of $m$ turned soft, plastic, and transparent. The gelation was an irreversible evolution for all samples, i.e., it could not be reverted by dissolution in concentrated acid solutions. This indicated that the polymers were ex-
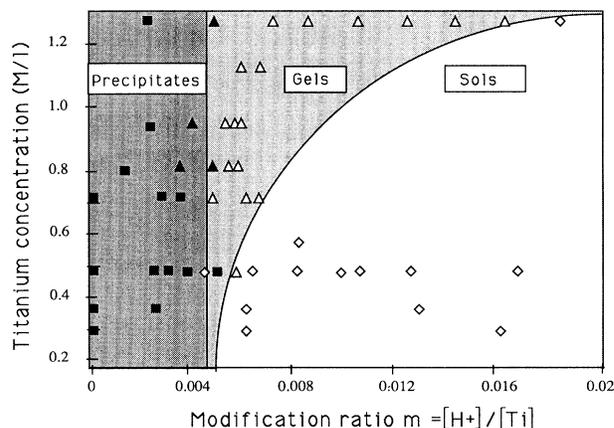


FIG. 2. Phase diagram for oxopolymers grown from Ti(OBu$^n$)$_4$ according to the modification ratio $m = [H^+][Ti]$ and to the concentration of Ti.

clusively oxopolymers.

At large values of $m$, the reactions were so slow that gelation did not occur within the time span of observation (about one year). All sols could be swollen in excess butanol, and then the polymer sizes, as measured through quasielastic light scattering, remained constant over time; this was taken as a further indication that condensation reactions are irreversible. The sol-gel boundary depends on time and alkoxide concentration; gel times are reported in the Results section.

### Final state of samples at stoichiometric hydrolysis

Samples prepared with larger amounts of water ($h = 4$) evolved much faster than those made at $h = 2$, and none of them remained sols. This made it possible to measure gel times $t_g$ over a wide range of concentrations; we found $t_g \approx [\mathrm{Ti}]^{-4}$.

Thus the final state of samples was determined by the three parameters concentration [Ti], hydrolysis ratio $h$, and inhibition ratio $m$. The effects of the first two are classical effects in sol-gel transitions [1–4]: larger hydrolysis ratios allow more extensive bridging, and higher monomer concentrations make it necessary to fill space better. The effect of inhibition is more remarkable in that different reaction conditions lead to different final states for samples with the same monomers hydrolyzed to the same extent.

## SMALL-ANGLE X-RAY SCATTERING (SAXS)

### Experimental method

The structures of the oxopolymers were investigated through SAXS. Experiments were performed on the instrument D22 of Laboratoire pour l'Utilisation du Rayonnement Electromagnétique (LURE) [21]; x rays of wavelength 1.2 Å were selected through a crystal monochromator and directed on the sample through a system of slits with point collimation; scattered rays were collected with a linear counter at distances selected at 1 or 2 m. Scattered intensities were measured according to the scattering vector $Q$; the complete range of $Q$ was from $Q = 0.5$ Å$^{-1}$ (distance $\approx 12$ Å) to $Q = 0.005$ Å$^{-1}$ (distance $\approx 1200$ Å).

### Data analysis for random structures

Most gels are random heterogeneous structures. As such they can be characterized by a finite set of geometrical parameters. First there must be some cutoffs: at short scales there is the size $a$ of the smallest heterogeneity, for instance, the distance between neighboring monomers; at long scales there is the size $\xi$ of the largest heterogeneities in the sample, for instance, a polymer size or a void size. Then there is the structure of these heterogeneities in the intermediate range of distances; this is described by the decay of correlations, i.e, the probability of finding a monomer at a distance $r$ if there is one at the origin. This decay can be exponential, as in the model of Debye and Bueche [22], or it may be a power law, as in fractal growth models. Because the oxopolymers result from a growth process it is likely that the correlations decay according to a power law; this decay is then characterized by an exponent $d_f$ which is analogous to a fractal dimension.

These parameters may be extracted from the scattering curves according to the behavior of the scattered intensity in three ranges of $Q$ values [23–25].

(1) At low values of $Q$ the scattering curves must follow the Guinier law; accordingly their curvature measures the size $\xi$ of the largest heterogeneities in the sample, and the magnitude of the scattered intensity yields the integrated content of these heterogeneities.

(2) At intermediate $Q$ values the intensity decays through interferences between monomers located at intermediate distances. Tenuous structures such as rods cause few interferences and yield a slow $Q^{-1}$ decay. Bushy structures with a fractal dimension $d_f$ yield a $Q^{-d_f}$ decay. Dense objects with a rough surface yield $Q^{-3}$ and dense objects with a smooth surface follow Porod's law with a $Q^{-4}$ decay.

(3) At high values of $Q$ the intensity reflects the correlations between neighboring monomers. If a monomer is fully coordinated to other monomers at a distance $a$, the resulting interferences will give a peak at a position $Q = 2\pi/a$, and the height of this peak will be related to the coordination number.

Sometimes these three ranges of $Q$ are not well separated; this is the case when there are less than two decades of distances between $\xi$ and $a$. Then, rather than determining the parameters according to separate ranges of $Q$ it is better to fit the whole scattering curve with an interpolation formula. This formula must reproduce the Guinier law at low $Q$ [23–25], and the power-law decay at high $Q$; the general form is [26]

$$\frac{I(Q)}{I(0)} = \left[ 1 + \frac{\sum\limits_{s=1}^{n} c_s (Q\xi)^{2s}}{(3d_f/2)} \right]^{(-d_f/2n)} . \tag{7}$$

The Guinier law imposes $c_1 = 2n/3d_f$ in every case. The higher-order terms differ according to the detailed shape of the heterogeneities; the first four have been determined for reaction-limited cluster aggregates (RLCA) [26], and the resulting crossover is sharper than that given by more widely used analytical forms [27]. In the absence of $a$ $priori$ knowledge on the shapes of the heterogeneities we chose to retain the first-order term only. Then expression (7) reduces to the older Fisher-Burford approximation [28] in a modified form where the correlation length $\xi$ has the same expression as the radius of gyration of isolated objects:

$$\frac{I(Q)}{I(0)} = \left[ 1 + \frac{(Q\xi)^2}{(3d_f/2)} \right]^{(-d_f/2)} . \tag{8}$$

### Data analysis for nonrandom structures

Some gels do not appear completely random in their spatial organization. In the scattering curves this comes out as a depression at low $Q$ followed by a peak, indicat-

ing that there is some regularity in the distribution of voids and lumps. This is particularly obvious on gels which are close to the precipitation boundary, as shown in Fig. 3. Similar observations were made through neutron scattering [2] and through light scattering [3] for oxopolymers made from silicon alkoxides. In these cases the polymers were examined before the gel point, and it was possible to dilute them in order to separate individual polymers. Spectra of the dilute samples did show that the depression had filled up, and that the ratios of intensity to concentration were much higher than for the undiluted samples. Hence the depression and the peak result from interferences between neighboring polymers. In this section we discuss how such interferences may be modeled.

For monodisperse spherical particles at a finite concentration $c$ the scattered intensity may be decomposed in terms which describe interferences within a particle and terms which describe interferences between particles [23–25]. The single-particle form factor $P(Q)$ is the square of the single-particle amplitude $A(Q)$:
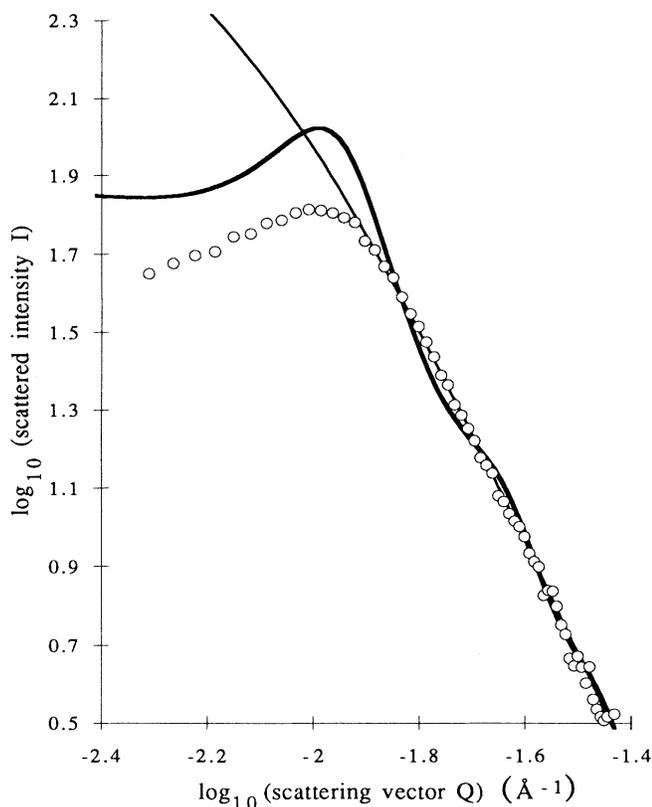
$$P(Q)=|A(Q)|^2 . \tag{9}$$



FIG. 3. Analysis of the scattering curves of gels according to a nonrandom packing of fractal objects. Circles: scattering curve of a gel made at the edge of the precipitation boundary, at $h=2$, $[Ti]=0.48M$, and modification ratio $m=0.0055$. Thin line: fit by the form factor of isolated fractal polymers, according to Eq. (8), with fractal dimension $d_f=3$ and cutoff $\xi=320$ Å. Thick line: fit by the scattering function of the same fractal aggregates, concentrated to a volume fraction of 0.25.

The interparticle structure factor $S(Q)$ is defined as Fourier transform of the pair distribution function $g(r)$:

$$S(Q)=1+c\,\mathcal{T}_F[g(r)-1] . \tag{10}$$

The resulting intensity may then be calculated as

$$I(Q)=cP(Q)S(Q) . \tag{11}$$

The main difficulty is the calculation of $g(r)$, for which some assumptions must be made. A classical procedure is to assume a hard-sphere potential, and obtain the pair correlation though an integral equation [29]. A fit made according to this procedure is shown in Fig. 3.

It appears that the simulation according to Eq. (11) produces a stronger oscillation of the scattering curve than that observed experimentally. This discrepancy indicates that correlations in the model are stronger than in reality. The origin of this discrepancy is that the oxopolymers which grow in the reaction bath are neither spherical nor monodisperse in sizes; the resulting distribution of distances smears out correlations to a large extent. We suspect that a similar situation occurs in many other gels, where the main feature in small-angle scattering is not a peak but a very sharp crossover from the Guinier regime to the fractal regime. Indeed, for all gels, the scattering at small $Q$ must be dominated by interferences between rays scattered by neighboring polymers, and these will depend on the relative sizes of the polymers.

It is therefore necessary to take into account the distribution of polymer sizes. Let $c_i$ be the concentration of polymers of class $i$, $A_i(Q)$ be the amplitude scattered by one of these polymers, and $g_{ij}(r)$ be the distribution function which describes their correlations in the presence of all other polymers. Then the structure factor of the mixture may be written as

$$S_{ij}(Q)=\delta_{ij}+\sqrt{c_i}\sqrt{c_j}\,\mathcal{T}_F[g_{ij}(r)-1] \tag{12}$$

and the scattered intensity is

$$I(Q)=\sum_{i,j}\sqrt{c_i}\sqrt{c_j}\,A_i(Q)A_j(Q)S_{ij}(Q) . \tag{13}$$

Here the problem is with the distribution of polymer sizes, which is known only for a small number of systems [30], and not for the titanium oxopolymers. For a real distribution the calculation is not possible, since there is an infinitely large number of species. We have calculated the scattered intensity for a distribution containing only three classes of polymers, and compared it with the intensity scattered by a gel which appears to show a suspiciously sharp crossover (Fig. 4). The agreement is much better than either the simulation made with no correlations between polymers or with interactions between monodisperse polymers. This indicates that correlation between neighboring polymers are important, but that they are partially smeared out by their size distribution.

### Results

*Low hydrolysis, low Ti concentration.* Figure 5 shows the experimental scattering curves for reaction baths made at $[Ti]=0.48M$ and $h=2$ with different values of
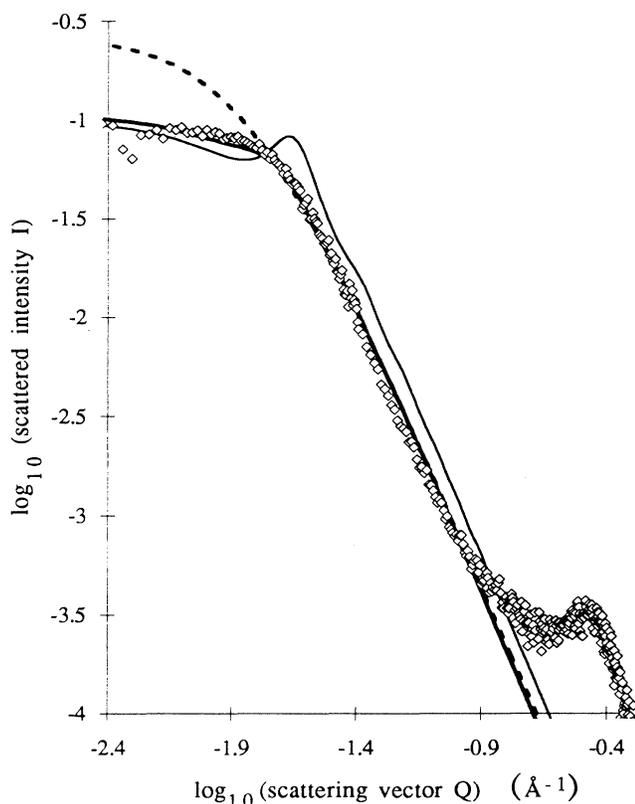
FIG. 4. Analysis of the scattering curves of gels made of concentrated polydisperse polymers. Squares: measured intensities. Full line: Simulation with polymers of three sizes and repulsive interactions between all of them. Thin line: same with polymers of one size only. Dotted line: no interactions between polymers.



FIG. 5. Scattering curves of oxopolymers made at $h=2$, $[Ti]=0.48M$, and different modification ratios; from top to bottom: $m=0.0055$, 0.0062, 0.01, 0.017, and 0.03. The peak or the curvature at low $Q$ correspond to a distance $\xi$ between polymers; the subsequent slope $d_f$ reflects their internal structure. Values of $\xi$ and $d_f$ extracted from the curves are listed in Table I.

the modification ratio $m=[H^+]/[Ti]$. The two uppermost curves correspond to transparent gels near the precipitation threshold. They show a peak at $Q=0.01$ Å$^{-1}$, distance $2\pi/Q=600$ Å, radius $\pi/Q=300$ Å, followed by a power-law decay over three decades in intensity and one decade in $Q$ vectors. The exponent is $-2.9$, indicating that the polymers are nearly dense. The middle curve is from a transparent gel in the middle of the $p$H range; here the cutoff at low $Q$ corresponds to a radius of 200 Å and the slope has decreased to $-2.8$. The two lowest curves are from samples made at high modification ratios, which were still sols after a reaction time of 12 months; the sizes are small, and the range of power-law decay is restricted; for this reason the internal structure of the polymers was determined through a fit of the scattering curve to the interpolation formula (8).

At this point it is appropriate to compare both procedures for estimating the sizes of heterogeneities and the fractal dimensions, i.e., peak position and straight line slope, or fit through the interpolation formula (8). The comparison is possible for the upper two curves of Fig. 5; here the fractal dimension $d_f$ is $-3$ according to the slope and $-2.9$ according to the fit; the radius $\xi$ of heterogeneities is 280-300 Å according to the peak posi-

tion and 240-280 Å according to the fits. The results from both procedures are similar, presumably because dense objects packed near contact give a distance (peak position) which is related to their radius. Accordingly, it was judged that the precision of the data did not warrant a more elaborate fit with the assumption of a particular distribution of polymer sizes, as in Eq. (13). Values of $\xi$ and $d_f$ measured according to the simpler fit, Eq. (8), are listed in Table I.

*Low hydrolysis, high Ti concentration.* Figure 6 shows the scattering from samples made at $[Ti]=0.98M$. Here as well samples prepared at high values of $m$ give large intensities and steep slopes, indicating that the polymers

TABLE I. Oxopolymers made at $[Ti]=0.48M$, $h=2$, and different modification ratios $m$: scattering exponent $d_f$ and radius $\xi$ (in Å) of the largest heterogeneities in the gel, from SAXS experiments.

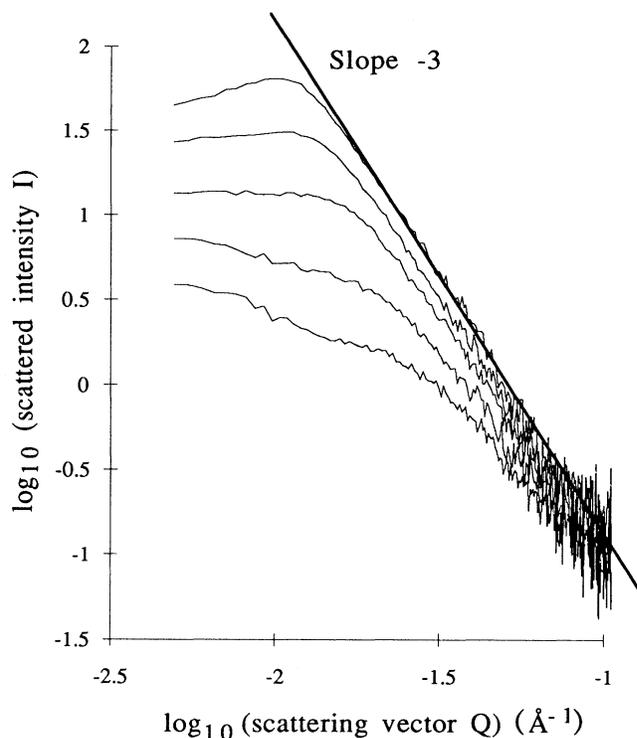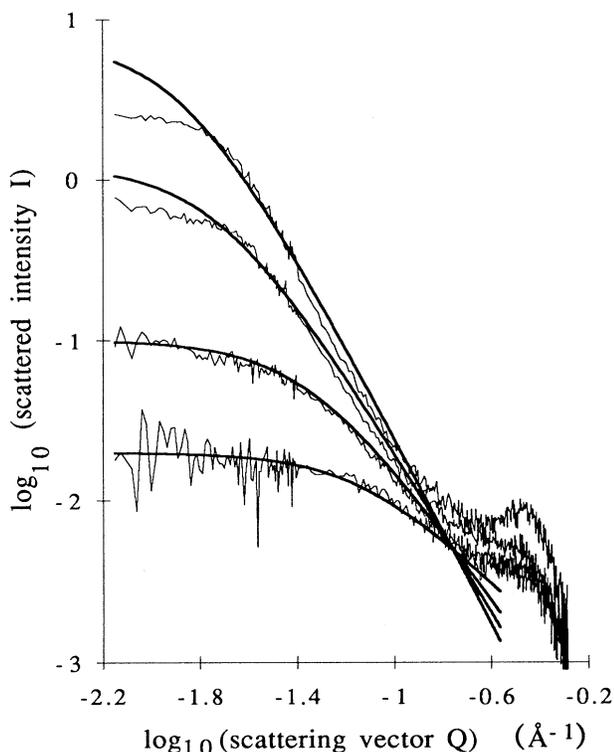| $m=[H^+]/[Ti]$ | $d_f$ | $\xi$ | Nature |
|---|---|---|---|
| 0.03 | 2.1 | 85 | Gel |
| 0.017 | 2.5 | 100 | Gel |
| 0.01 | 2.8 | 200 | Gel |
| 0.0062 | 2.9 | 240 | Turbid gel |
| 0.0055 | 3 | 280 | Turbid gel |

FIG. 6. Scattering curves of oxopolymers made at $h=2$, $[\text{Ti}]=0.98M$, and different modification ratios, from top to bottom: $m=0.007, 0.01, 0.018$, and $0.025$. The full lines are fits to the data according to the Fisher-Burford approximation. Values of $\xi$ and of $d_f$ extracted from the curves are listed in Table II.

are large and nearly dense; samples prepared at low values of $m$ give low intensities and weak slopes, indicating that the polymers are small and tenuous. However, the range of self-similar behavior is more limited because of the higher concentration; this is because the polymers are closer together, hence the size $\xi$ of the largest heterogeneities must be shorter. These values are listed in Table II.

At the high-$Q$ end, these spectra show a peak corresponding to the repetition of subunits within a polymer; the distance is comparable with the distance between tri-

TABLE II. Oxopolymers made at $[\text{Ti}]=0.98M$, $h=2$, and different modification ratios $m$: scattering exponent $d_f$ and radius $\xi$ (in Å) from SAXS.

| $m=[\text{H}^+]/[\text{Ti}]$ | $d_f$ | $\xi$ | $t_g$ |
|---|---|---|---|
| 0.032 | 1.5 | 30 | 19 month |
| 0.025 | 1.9 | 30 | 19 month |
| 0.018 | 2.1 | 40 | 7 month |
| 0.016 | 2.2 | 100 | 3 month |
| 0.012 | 2.4 | 100 | 2 d |
| 0.010 | 2.5 | 100 | 6–12 h |
| 0.0084 | 2.7 | 100 | 120 min |
| 0.007 | 2.9 | 110 | 15 min |
| 0.0047 | 2.9 | 120 | 7 min |
| 0.0021 | 3 | >1000 | precipitates |

mers in the precursor, therefore these subunits may be trimers as well. The height of the peak decreases at higher modification ratio $m$, hence the coordination number of a subunit in the chain is high near the precipitation boundary and low in very acidic conditions. The same peak would have been observed in all other experiments if the $Q$ range of the instrument had been extended far enough.

*Stoichiometric hydrolysis.* Similar effects were observed for reactions made at larger hydrolysis ratios, but the effects of modification were less pronounced. Figure 7 shows spectra obtained at $h=4$. At low modification ratios (upper curves) the small-$Q$ part of the curves shows a slight peak, and the position of this peak does not change with concentration; as above, this indicates that the gel is made of dense polymers with a radius around 300 Å; the peak position is the distance of closest approach between polymers. At high modification ratios the peak vanishes and the scattering curves are typical of bushy, interpenetrated polymers. The values of $\xi$ and $d_f$ extracted from these scattering curves according to Eq. (8) are presented in Table III.

*Concentration effects* were investigated for gels prepared at low $m$, near the precipitation threshold. In this case the scattering curves of all gels are identical regardless of Ti concentration: all of them show a peak at
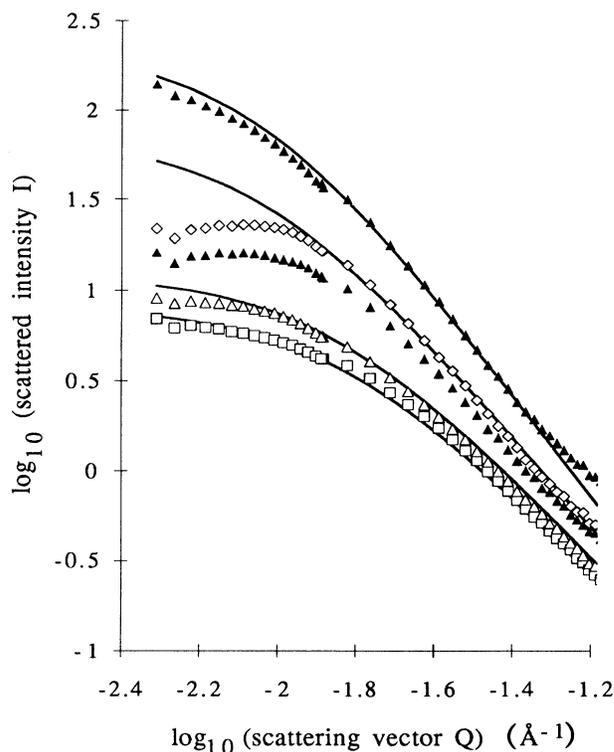


FIG. 7. Scattering curves of oxopolymers made at $h=4$, $[\text{Ti}]=0.48M$, and different modification ratios; from top to bottom: $m=0.008, 0.021, 0.024, 0.033$, and $0.061$. The peak or the curvature at low $Q$ correspond to a distance $\xi$ between polymers; the subsequent slope $d_f$ reflects their internal structure. Values of $\xi$ and of $d_f$ extracted from the curves are listed in Table III.

TABLE III. Oxopolymers made at $[Ti]=0.48M$, $h=4$, and different modification ratios $m$: scattering exponent $d_f$ and radius $\xi$ from SAXS.

| $m$ | $d_f$ | $\xi$ | Nature |
|---|---|---|---|
| 0.061 | 2.3 | 127 | Gel |
| 0.033 | 2.3 | 135 | Gel |
| 0.024 | 2.5 | 200 | Gel |
| 0.021 | 2.6 | 210 | Gel |
| 0.016 | 2.6 | 210 | Gel |
| 0.008 | 3 | 240 | Precipitate |
| 0.006 | 3 | 240 | Precipitate |

$Q=0.012$ Å$^{-1}$ followed by a steep decay with an exponent $-2.9$. Hence the gels appear to be made of the same dense polymers with the same distances between them. Presumably large voids must also be present in the gels made at low concentrations, but these are not visible in the $Q$ range of the experiment.

In summary, the results show a continuous variation of the structures according to the inhibition ratio $m$. These structures have a large range of self-similar correlations, as do fractal structures, but the exponents which describe these correlations do not have the universal values predicted by aggregation models (e.g., $d_f=2.1$ for RLCA). Similar information is provided by the peak at the high-$Q$ end of the small-angle scattering curves, indicating that the coordination number of subunits in the oxopolymers increases continuously as the precipitation limit is approached. Still, these results do match the observed macroscopic behavior of the samples, which give transparent gels for samples made of polymers with $d_f=2$, turbid gels at higher $d_f$, and precipitates at $d_f=3$.

## DISCUSSION

The system studied here, and the results presented above, are representative of problems generally encountered in sol-gel science. Indeed, this field may be defined as the application of growth processes to the fabrication of materials. In the present case, growth processes have been performed through condensation of monomers dispersed in a solvent; the problem is that different reaction conditions select different reaction paths and yield different final states of the material. These final states have been classified according to their macroscopic properties (sols, transparent gels, turbid gels, precipitates). They have been further characterized according to small-angle scattering results. Both types of observations point to a systematic relation between the reaction conditions and the final state of the system. This justifies *a posteriori* the empirical methods used by previous workers for the control of the materials; however, it does not solve the basic problem, which can be restated as follows.

*(1) Structures.* How many different final states are there, that is, final states which differ in statistical properties such as correlations in the spatial distribution of monomers and connectivity for the resulting polymers?

*(2) Growth modes.* How many different growth modes are necessary to generate the final states? Can these

growth modes be rationalized according to known physical processes, as is usually done in this field, or is it necessary to inject some chemical rules into the line of reasoning, as suggested by those of our colleagues who are designing new materials?

### Structures

Small-angle scattering curves reveal a systematic variation of structures according to reaction conditions. Indeed gels made at low modification ratios, near the precipitation threshold, yield large scattered intensities, correlation peaks in the 600-Å range, and steep intensity decays at high $Q$; gels made at high modification ratios, away from the precipitation boundary, yield low intensities, Guinier-type curvature followed by a slow decay of intensity. In order to turn this comparison into a precise structural description it is necessary to identify the objects which cause the scattering and to determine the correlations between the relative positions of these objects in the sample.

In small-angle scattering such a description may be obtained if the decay of intensity is analyzed into (i) interferences between pairs of scatterers which belong to the same object, and (ii) interferences between pairs which belong to distinct objects. It is expected that interobject interferences dominate at large distances (low $Q$) and intraobject interferences at short distances (high $Q$). For this reason it is much easier to first analyze the local arrangements of subunits and then proceed to their large scale distribution.

(a) At very short scales (high $Q$) the main feature is the peak corresponding to *distances between neighboring subunits* (Figs. 4 and 7). The position of this peak is similar to that of the peak in precursor solutions (the distance equals 15 Å in this case), hence it is likely that the subunits are trimers or dimers which were bridged to each other during polymerization. The peak height is related to the number of neighbors at the same repetition distance. Here gels made at low $m$ show large peaks, indicating that each subunit has a nearly full coordination shell, as in dense structures; in gels made at high $m$ the peak is weak, as in polymeric structures with a low coordination number [31].

(b) At intermediate scales there is a power-law decay of intensity which reflects the *spatial distribution of subunits in a polymer*. For samples prepared at low-$m$ values the power-law behavior extends over one decade in $Q$ values and three decades in intensity; the exponent $d_f$ is $-3$. This exponent indicates that the polymers are dense objects with a rough surface. Consequently, as they become macroscopic, they do not invade the whole sample volume; this is in agreement with the observation that such samples are near the precipitation boundary. For samples prepared at high-$m$ values the range of power-law behavior is more limited, and the exponent $d_f$ lies between $-2$ and $-3$. Such structures entrap the whole sample volume as they become macroscopic; this is in agreement with the observation that these samples become gels at a sufficient reaction time.

(c) At large scales the main feature is the saturation of intensity, which reflects the content and the size of the *largest heterogeneities in the sample*. For samples made at low-$m$ values near the precipitation boundary, the intensity saturates at very high values, indicating that the heterogeneities are massive objects. The location in $Q$ of this saturation (peak at $Q = 0.01$ Å$^{-1}$ corresponding to distances of 600 Å) indicates that such heterogeneities have radii $\xi$ on the order of 300 Å. This size does not depend on concentration; therefore it is also, in this case, the size of polymers which are not interpenetrated.

For samples prepared at high-$m$ values, the saturation values of intensity are much smaller and the curvature at low $Q$ yields a length $\xi$ which is rather short. The intensities become even lower and the lengths even shorter when the overall concentration is raised. Therefore this must be another effect of interferences between polymers, where long-wavelength fluctuations are suppressed more efficiently at high polymer concentration. As in semidilute polymer solutions, such fluctuations are more easily described as voids between polymer strands. Accordingly the size $\xi$ of heterogeneities is the radius of larger voids in the mesh of interpenetrated polymers.

(d) Now we can try to build structural models by putting together the information collected at the three different length scales. In *samples made at low-$m$ values* the polymers are dense on a local scale (peak at high $Q$) and at intermediate scales ($Q^{-3}$ decay), although they have a rough surface. At larger scales the structure contains lumps and voids with regular spacings of about 600 Å regardless of concentration; this implies that the polymers grow dense and monodisperse up to radii of 300 Å, then bind to each other to form dense flocs. In *samples made at high-$m$ values* the polymers are bushy objects with a low coordination number (no peak at high $Q$) and voids at all intermediate scales (scattering exponent between $-2$ and $-3$). At larger scales the size of the largest voids or lumps depends on concentration ($\xi$ varies between 30 and 100 Å); hence the voids of larger polymers must be penetrated by smaller polymers.

Thus in this growth problem there is a relation between internal structure and interpolymer correlations. Depending on the $m$ ratio the growth may produce either dense monodisperse polymers which do not overlap or bushy polydisperse ones where the smaller ones fill the voids of larger ones. Now it is necessary to examine what may be the cause of this switch in the growth mode.

### Growth modes

The switch from *fractal growth* (at high $m$) to *dense growth* (at low $m$) is surprising because throughout this range of conditions the condensation reactions are always irreversible. It is well known that the recombination of polymers through irreversible reactions yields bushy structures [32]. Because bushy objects of comparable sizes cannot interpenetrate, each recombination will create voids of sizes comparable to the polymer sizes and therefore the structures will be self-similar; for low reaction probabilities the self-similarity exponent is close to 2 (this is the RLCA model) [32].

*Dense growth* cannot result from irreversible recombination reactions between polymers of comparable sizes. Now the reactions are certainly irreversible, as this has been checked through dilution experiments before the gel point and through attempts to redissolve the gel in concentrated acids. Thus *the only way out is that the reactions should be between small and large polymers.* Indeed if the reactivity of small polymers is low they can penetrate into voids of the larger ones and react there; this leads to densification of the larger polymers [31].

However, a selection of small plus large reactions cannot occur for physical reasons alone; indeed under RLCA conditions it has been found that there is no net transfer between the populations of small, middle, and large polymers [30]. In the present case changes in the $m$ ratio do modify the *overall reactivity;* this effect alone does not change the relative frequencies of small plus small, small plus large, and large plus large reactions. Thus a shift to dominant small plus large reactions can only result from a change in the *differences in reactivity* between small and large polymers.

Such differences in reactivity may indeed result from differences in the chemical environment of the titanium atoms in these polymers. Indeed, as mentioned in the section on "chemical reactions," successive oxolation reactions on the same Ti are favored at low $m$. This *feedback loop* between chemical environment and reactivity is enough to cause a switch in the growth mode. Indeed the first monomers [33] to condense become more reactive than all others; hence the first polymers recombine together to form large structures and they leave aside a large pool of unused, less reactive monomers. Later, because *the reservoir is finite*, these monomers must be used and the dominant reactions become small plus large reactions. Thus a switch to densification must occur if uncondensed monomers are the least reactive species, and are used at the end of growth; if this switch occurs sufficiently early the polymers become fully dense and precipitate.

We have devised a numerical model which simulates the condensation of multifunctional monomers in situations where there are differences of reactivity according to the number of functions already reacted [31]. These differences are described by a reactivity function

$$f(v_i) = w^{v_i} , \tag{14}$$

where $v_i$ is the number of functions already reacted by monomer $i$ and $w$ is a parameter which measures the strength of the feedback between coordination and reactivity. Values of $w$ which are above unity indicate that monomers which have already reacted become more reactive, whereas values of $w$ which are below unity indicate that monomers become inhibited after having reacted.

For high enough values of $w$ the model shows a first stage where a few dimers are formed, a second stage where these dimers recombine to form large bushy polymers, and a last stage where these polymers capture all the unused monomers. The onset of the last stage depends on the strength of the feedback parameter $w$; if

$w \geq 2$ most monomers are added during this last stage; because the dense regions of the large polymers are the most reactive the monomers fill up all their voids. Consequently dense polymers are obtained at $w \geq 2$. At lower values of $w$ a continuous range of less dense structures is obtained; the calculated scattering curves of these polymers are presented in Fig. 8; they should be compared with the experimental curves presented in Figs. 4–7.

This comparison can be made more quantitative by selecting experimental and theoretical scattering curves which yield the same scattering exponent $d_f$. The theoretical scattering curve is determined by the choice of the model parameter $w$ which measures the strength of chemical feedback for the condensation of monomers; the experimental curve is determined by the value of the ratio $m$ which measures the strength of selective inhibition of oxolation reactions. The values of $w$ and $m$ which give matching scattering curves are presented in Fig. 9. This comparison can be analyzed as follows.

(i) At low inhibition ratios ($m \leq 0.005$), dense polymers ($d_f = 3$) are obtained in all experiments. They are reproduced with values $w \geq 2$ of the model parameter. Consequently the comparison starts at the point $m = 0.005$, $w = 2$.

(ii) At intermediate inhibition ratios ($0.0005 < m < 0.015$) the polymers are bushy objects with scattering
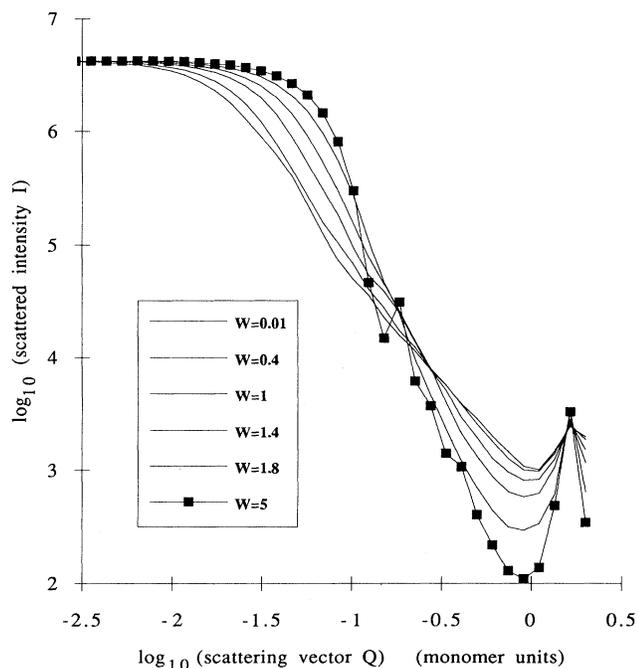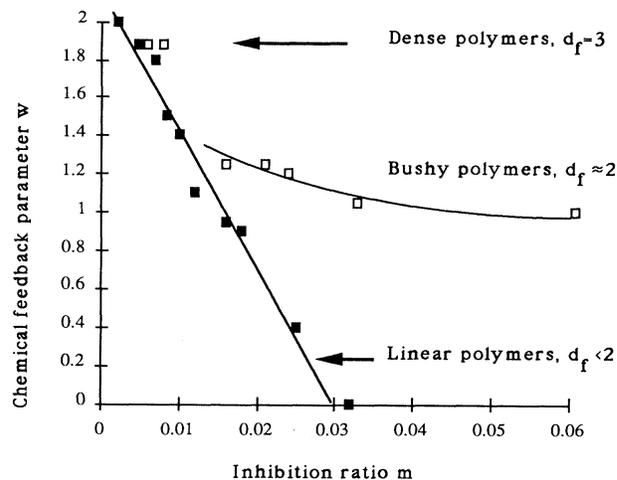


FIG. 9. Values of the chemical feedback strength $w$ which are used to reproduce the scattering from gels made at various inhibition ratios $m$. The parameter $w$ determines in the model how the reactivity of monomers changes with the number of functions they have already reacted. The inhibition ratio $m = [H^+]/[Ti]$ determines in the experiment which condensation reactions are most likely. Each point in the figure corresponds to a model ($w$) and an experiment ($m$) which give the same scattering exponent $d_f$. The filled squares correspond to experiments performed at low hydrolysis ($h = 2$) and the open squares to experiments performed at stoichiometric hydrolysis ($h = 4$).



FIG. 8. Scattering curves calculated for model polymers constructed at different values of the chemical selection parameter $w$. The curvature at low $Q$ describes the overall sizes and shapes of the polymers: tenuous polymers have larger radii, hence the downward curvature is at lower $Q$; dense polymers have small radii, and the curvature is sharp because it reflects the particle shape oscillations, as in a dense sphere. The slope at higher $Q$ describes the internal structure of the polymers, and the peak at the high-$Q$ end corresponds to nearest-neighbor distances between monomers.

exponents $d_f$ between 2.3 and 2.5. They are reproduced with values $1.2 < w < 2$ of the model parameter, with a one-to-one correspondence between the values of $m$ and those of $w$, regardless of other reaction conditions such as the hydrolysis ratio $h$. In this range the growth is well described by a process where branched polymers densify by capturing monomers.

(iii) At high inhibition ratios ($m > 0.015$), the structures of the polymers depend on the hydrolysis ratio. At low hydrolysis ratios (filled squares), the polymers are mostly linear (exponents below 2); this is easily understood since there is not enough water for extensive branching. These polymers are reproduced by models where $w$ is below unity, which yields a low probability for further condensation reactions. At large hydrolysis ratios (open squares), the experiments indicate that the polymers are still bushy objects. This is understood since there is nothing that discourages branching: enough water is available for extensive branching, and any differences in reactivity have been swamped by the strong inhibition. This is the RLCA behavior, which is reproduced by the model with $w = 1$.

This comparison shows that a model where monomers and oligomers condense according to a chemical feedback rule can reproduce the main features of the growth of polymers in sol-gel processes, and in particular their scattering exponents $d_f$. It cannot, however, explain features which depend on the distances between growing polymers, which determine the sizes of heterogeneities in the final material.

These features are of two types. For bushy, interpenetrated polymers, the size of heterogeneities is determined by the distance between strands of neighboring polymers. Description of this interpenetration would require a model where the spatial relations of neighboring polymers are taken into account, which would be a formidable task. For dense polymers the size of heterogeneities appears to be constant; it must be determined in the early stage of growth, where polymers can recombine only if they are not too far apart; then densification through capture of unused monomers takes over and produces finite lumps. Again, description of this competition between recombination and densification would require a model where the spatial relations of polymers are taken into account.

## CONCLUSIONS

Sol-gel chemistry depends on growth processes to produce materials which are dispersed at the nanometer scale. Classical growth processes are *stationary* in that the same type of recombinations are performed throughout the growth. A good example is the early growth of silica polymers in solutions of silicon alkoxides: there the distribution of polymer sizes propagates similarly to itself at larger and larger scales until the polymers invade the whole volume [30]. As a result, the polymer structures are also self-similar, and in this case they are fractals with an exponent $d_f \approx 2$. This is the universal result for recombination of polymers through irreversible reactions.

In this work we have shown that the growth of oxopolymers from Ti alkoxides leads to nonuniversal results: we observed a crossover from gelation to precipitation, and we have shown that this crossover reflects a continuous change in polymer structures from bushy to dense.

The occurrence of dense structures cannot result from regular nucleation and growth processes where nondense branches would be destroyed by reverse reactions, because all condensation reactions are irreversible. We have proposed that, instead, dense growth in transition-metal alkoxides occurs through a two-stage growth process where a few large polymers grow first, and then they densify through capture of unused monomers. This growth process is *nonstationary*.

As with other nonstationary reactions, two ingredients

must be present: *differentiation* of species according to their chemical buildup, and *sequential use* of the most reactive, and later the least reactive species. We have shown that the *dense growth* of oxopolymers from Ti alkoxides occurs precisely when these two conditions are met: differentiation because oxygens in oxo bridges are more acidic, and therefore less inhibited than others; sequential use because these more reactive groups are used first in the recombination of oxopolymers, while the remaining, uncondensed monomers are used only later, causing densification of the oxopolymers.

The results of such nonstationary growth processes depend on the relative importances of the recombination (large plus large) and densification (small plus large) stages of the growth process. For alkoxides at large concentration of inhibitors such as $H^+$ differentiation is weak; consequently most of the growth proceeds through recombination, and densification occurs only at the end, causing a modest increase in $d_f$ above its universal value. At low concentration of inhibitors, and especially for transition-metal alkoxides, differentiation is quite strong; consequently a small fraction of the monomers condense together to form a small number of oxopolymers; this recombination stage is short, and the densification which follows it is extensive; this results in precipitation.

It is highly likely that such chemical selection operates to some extent in all processes where multifunctional monomers are dissolved in a solvent and condensed into polymers. Thus is it quite possible that most materials made through sol-gel processes are hybrids which result from a combination of early fractal growth and later densification; indeed many of the so-called "fractal" dimensions measured at the end of all reactions in a sol-gel process are above the RLCA value of 2.1. If this is true, then none of these materials are true fractals. Conversely, we have demonstrated that nonuniversal values of the scattering exponent may be caused by nonstationary growth modes.

## ACKNOWLEDGMENTS

[1] C. J. Brinker and G. Scherer, *Sol-Gel Science* (Academic, San Diego, 1989).

[2] B. Cabane, M. Dubois, and R. Duplessix, J. Phys. (Paris) **48**, 2131 (1987).

[3] M. Dubois and B. Cabane, Macromolecules **22**, 2526 (1989).

[4] B. Cabane, M. Dubois, F. Lefaucheux, and M. C. Robert, J. Non-Cryst. Solids **119**, 121 (1990).

[5] B. E. Yoldas, J. Mater. Sci. **21**, 1086 (1986).

[6] M. Kallala, C. Sanchez, and B. Cabane, J. Non-Cryst. Solids **147**, 189 (1992).

[7] D C. Bradley, R. C. Mehrotra, and D. P. Gaur, *Metal Alkoxides* (Academic, New York, 1978).

[8] S. Doeuff, M. Henry, C. Sanchez, and J. Livage, J. Non-Cryst. Solids **89**, 206 (1987).

[9] C. Sanchez, J. Livage, M. Henry, and F. Babonneau, J. Non-Cryst. Solids **100**, 650 (1988).

[10] J. Livage, M. Henry, and C. Sanchez, Prog. Solid State Chem. **18**, 259 (1988).

[11] C. Sanchez and J. Livage, New J. Chem. **14**, 513 (1990).

[12] F. Babonneau, S. Doeuff, A. Leaustic, C. Sanchez, C. Cartier, and M. Verdaguer, Inorg. Chem. **27**, 3166 (1988).

[13] C. Sanchez, F. Ribot, and S. Doeuff, in *Inorganic and Organometallic Polymers with Special Properties,* Vol. 206 of *NATO Advanced Study Institute, Series B: Physics,* edited by R. M. Laine (Kluwer, Dordrecht, 1992), p. 267.

[14] F. Ribot and C. Sanchez (unpublished).

[15] C. Sanchez, M. In, P. Toledano, and P. Greismar, in *Better Ceramics Through Chemistry V,* edited by M. J. Hampden-Smith, W. G. Klemperer, and C. J. Brinker, MRS Symposia Proceedings No. 271 (Materials Research Society, Pittsburgh, 1992), p. 669.

[16] T. J. Bastow, M. E. Smith, and H. J. Whitfield, J. Mat. Chem. **2,** 989 (1989).

[17] A. N. Nemesyanov, E. M. Brainina, and R. K. Freidlina, C. R. Dokl. Acad. Sci. URSS **85,** 571 (1952).

[18] T. Boyd, J. Polym. Sci. **7,** 591 (1951).

[19] G. Winter, J. Oil Colour Chem. Assoc. **36,** 699 (1953).

[20] T. Hiemstra, J. C. M. De Wit and W. H. Van Riemsdijk, J. Colloid Interface Sci. **133,** 91 (1989); **133,** 105 (1989).

[21] J. M. Dubuisson, J. M. Dauvergne, C. Depautex, P. Vachette, and C. E. Williams Nucl. Instrum Methods Phys. Res. A **246,** 636 (1986).

[22] P. Debye and A. M. Bueche, J. Appl. Phys. **20,** 518 (1949).

[23] A. Guinier and G. Fournet, *Small Angle Scattering of X Rays* (Wiley, New York, 1955).

[24] O. Glatter and O. Kratky, *Small Angle X Ray Scattering* (Academic, New York, 1982).

[25] B. Cabane, in *Surfactant Solutions: New Methods of Investigation,* edited by R. Zana (Dekker, New York, 1987), p. 57.

[26] M. Y. Lin, R. Klein, H. M. Lindsay, D. A. Weitz, R. C. Ball, and P. Meakin, J. Colloid Interface Sci. **137,** 263 (1990).

[27] J. Teixeira, in *On Growth and Form,* edited by H. E. Stanley and N. Ostrowski (Nijhoff, Dordrecht, 1986).

[28] M. E. Fisher, R. J. Burford, Phys. Rev. **156,** 583 (1967).

[29] K. Hiroike, J. Phys. Soc. Jpn. **27,** 1415 (1969).

[30] Z. Grubisic-Gallot, F. Schosseler, F. Lixon, and B. Cabane, Macromolecules **25,** 3733 (1992).

[31] M. Kallala, R. Jullien, and B. Cabane, J. Phys. II France **2,** 7 (1992).

[32] R. Jullien and R. Botet, *Aggregation and Fractal Aggregates* (World Scientic, Singapore, 1987).

[33] In the following, the term "monomers" is used to designate the units which condense through oxolation, even though they may be olated oligomers.